AD-A123 991 ANALYSIS OF NON-PERIODIC SURFACE ACOUSTIC WAVE TRANSDUCERS AND REFLECTORS(U) ILLINOIS UNIV AT URBANA COORDINATED SCIENCE LAB A L LENTINE MAY 80 R-883 1/1

UNCLASSIFIED N00014-79-C-0424 F/G 9/1 NL

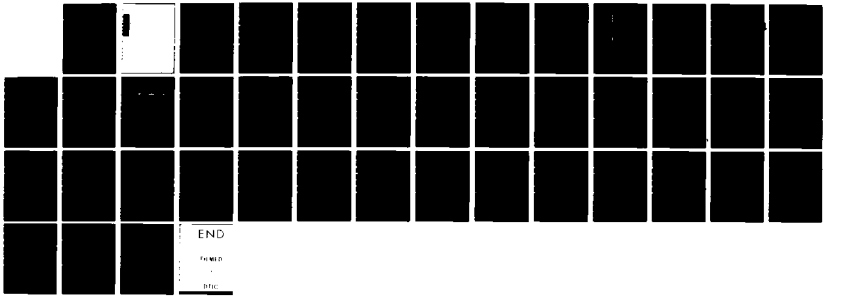

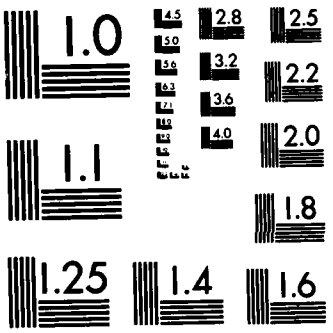

UILU-ENG 80-2215

ANALYSIS OF NON-PERIODIC SURFACE ACOUSTIC WAVE TRANSDUCERS AND REFLECTORS

by

Anthony L. Lentine

This work was supported in part by the Joint Services Electronics Program (U.S. Army, U.S. Navy and U.S. Air Force) under Contract N00014-79-C-0424 and in part by the U.S. Air Force under Contract F19628-78-C-0040.

UNCLASSIFIED

SECURITY CLASSIFICATION OF THIS PAGE *(When Data Entered)*

REPORT DOCUMENTATION PAGE		READ INSTRUCTIONS BEFORE COMPLETING FORM
1. REPORT NUMBER	2. GOVT ACCESSION NO. AD-A123991	3. RECIPIENT'S CATALOG NUMBER
4. TITLE *(and Subtitle)* ANALYSIS OF NON-PERIODIC SURFACE ACOUSTIC WAVE TRANSDUCERS AND REFLECTORS		5. TYPE OF REPORT & PERIOD COVERED Technical Report
		6. PERFORMING ORG. REPORT NUMBER UILU-ENG 80-2215
7. AUTHOR(s) Anthony L. Lentine		8. CONTRACT OR GRANT NUMBER(s) N00014-79-C-0424 F19628-78-C-0040
9. PERFORMING ORGANIZATION NAME AND ADDRESS Coordinated Science Laboratory University of Illinois at Urbana-Champaign Urbana, Illinois 61801		10. PROGRAM ELEMENT, PROJECT, TASK AREA & WORK UNIT NUMBERS
11. CONTROLLING OFFICE NAME AND ADDRESS Joint Services Electronics Program		12. REPORT DATE May, 1980
		13. NUMBER OF PAGES 37
14. MONITORING AGENCY NAME & ADDRESS *(if different from Controlling Office)*		15. SECURITY CLASS. *(of this report)* UNCLASSIFIED
		15a. DECLASSIFICATION/DOWNGRADING SCHEDULE

16. DISTRIBUTION STATEMENT *(of this Report)*

Approved for public release; distribution unlimited

17. DISTRIBUTION STATEMENT *(of the abstract entered in Block 20, if different from Report)*

18. SUPPLEMENTARY NOTES

19. KEY WORDS *(Continue on reverse side if necessary and identify by block number)*

Surface Acoustic Waves
Transducers and Reflectors

as presented

20. ABSTRACT *(Continue on reverse side if necessary and identify by block number)*

In this report, ~~I will present~~ a method to calculate the response of non-periodic surface acoustic wave transducers, and also a method that can be used to calculate the reflection and phase shift of non-periodic reflective arrays. The methods do not consider mechanical effects, so grooved reflector arrays can not be analyzed. However a large majority of surface wave devices can be analyzed using one or both of these two methods.

DD FORM 1 JAN 73 1473

SECURITY CLASSIFICATION OF THIS PAGE *(When Data Entered)*

ANALYSIS OF NON-PERIODIC SURFACE ACOUSTIC WAVE TRANSDUCERS AND REFLECTORS

BY

ANTHONY L. LENTINE

B.S., University of Illinois, 1979

THESIS

Submitted in partial fulfillment of the requirements
for the degree of Master of Science in Electrical Engineering
in the Graduate College of the
University of Illinois at Urbana-Champaign, 1980

Thesis Adviser: Professor B. J. Hunsinger

Urbana, Illinois

ACKNOWLEDGEMENT

I wish to thank Professor Bill J. Hunsinger for his help and encouragement throughout the preparation of this thesis. I also wish to thank Professor Supriyo Datta and Dr. Carl M. Panasik for their help with technical matters and Steve Wilkus for his help in computer programming.

TABLE OF CONTENTS

I. Introduction

In this thesis, I will present a method to calculate the response of non-periodic surface acoustic wave transducers and a method that can be used to calculate the reflection and phase shift of non-periodic reflective arrays. The methods do not consider mechanical effects, so grooved reflector arrays can not be analyzed. However a large majority of surface wave devices can be analyzed using one or both of these two methods.

The central problem in calculating the response of SAW interdigital transducers is to determine the charge distribution on the electrodes. In the weak coupling approximation, this charge distribution is calculated from the electrostatic field equations alone, neglecting piezoelectricity. It has been shown that the problem is simplified considerably for periodic transducers with arbitrary voltages by an application of the superposition principle [1,2,3]. Using this principle the spectral charge distribution can be found from the product of an array factor and an element factor. The array factor is the Fourier transform of the electrode voltages and the element factor is given by a known analytical expression [4]. However, for withdrawal weighted or chirped transducers, which are non-periodic, the electrostatic field equations must be solved anew for each individual transducer using the appropriate surface boundary conditions. Two approaches to this problem have been discussed in the literature, namely the Fourier transorm approach [5] and the Green's function approach [6,7]. Each of these approaches uses field theory.

The first part of this thesis describes a new approach based on a simple circuit model that yields accurate charge distributions for arbitrary non-periodic transducers. A non-periodic transducer is

approximated by a periodic transducer consisting of many small electrodes (figure 1). An electrode in the non-periodic transducer is replaced by many small electrodes that are connected together, while a gap is replaced by many small floating electrodes. This replacement is equivalent to a sampling process, and it is accurate if the small electrode spacing is much less than one wavelength at the frequency of interest. The potential distribution for the non-periodic transducer is given by the voltages on the small electrodes. Since the voltages on the floating electrodes are unknown they must be found using the circuit model. The transducer consisting of small electrodes is represented by a circuit whose nodes represent the electrodes. These nodes are connected by capacitors which represent the interelectrode capacitance (figure 2). For a periodic transducer, the values of these capacitors are given by an analytical expression [4]. The response of the transducer can be calculated from the charge distribution which is given by the charges on the small electrodes. These charges are found using the circuit model.

For reflective arrays of electrodes, it is important to know the reflection and phase shift of the surface waves as opposed to the response of the array due to an applied voltage. The most common method of determining the phase shift and reflection is to determine the reflection and velocity shift, which is related to the phase shift, of a single electrode in the array and then combine the effects of all of the electrodes. By velocity shift, I mean the difference between the velocity of the surface wave as it propagates under an electrode (assuming that the velocity in the gap is equal to the free surface velocity) and the velocity of a surface wave with no electrodes present. To calculate the reflection and velocity shift of surface waves from an electrode in an array one must

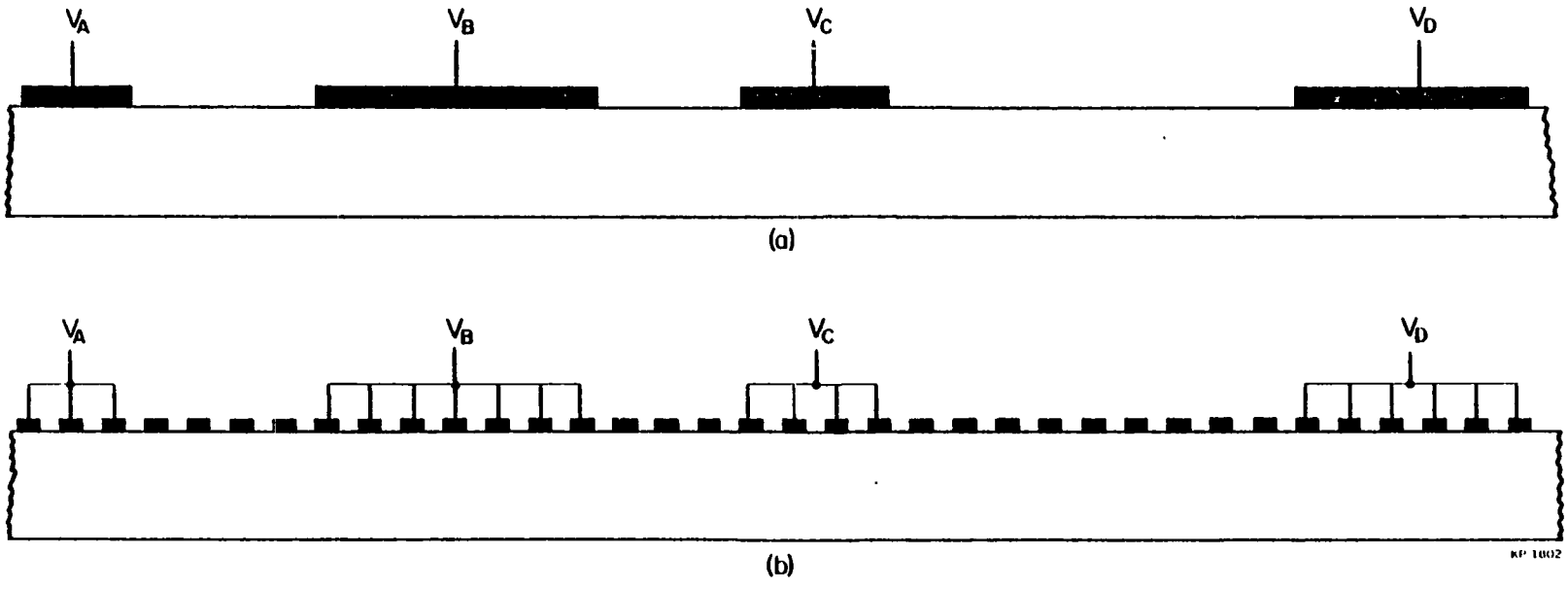

Figure 1: Non-periodic SAW transducer modeled with a periodic array of small electrodes.
(a) actual electrode
(b) modeling with small electrodes

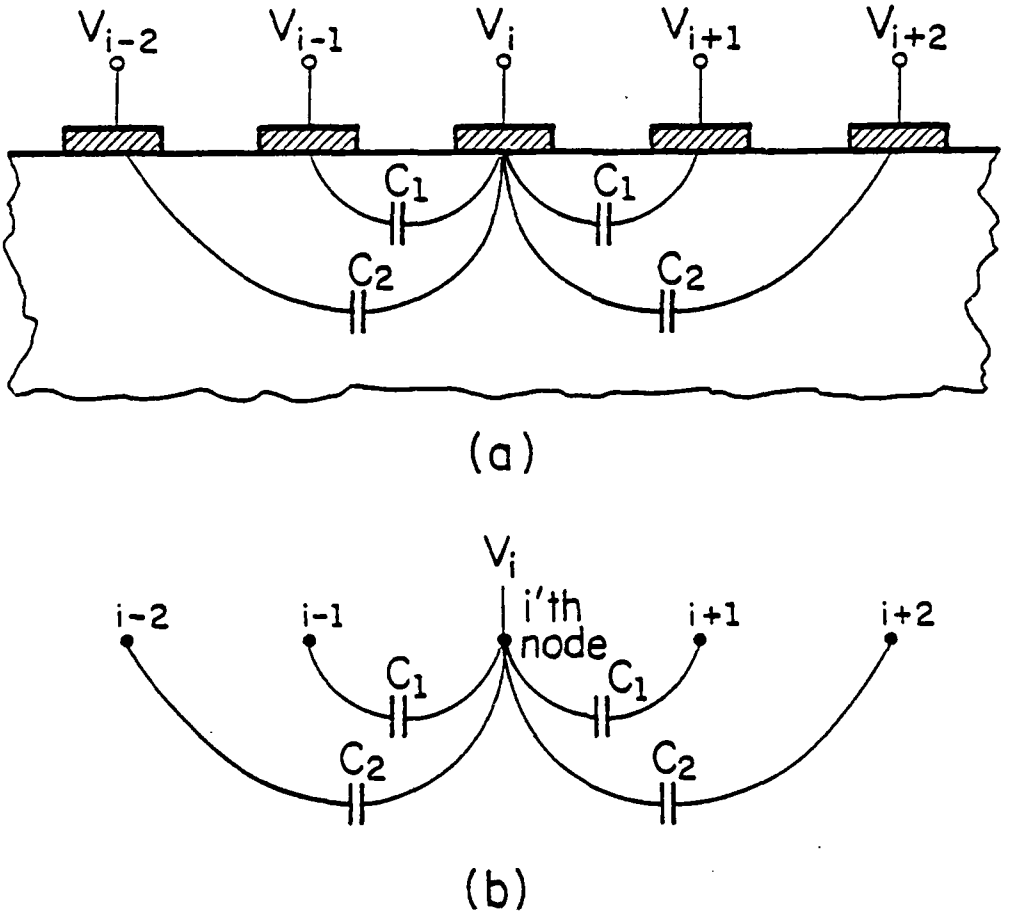

Figure 2: Transducer Capacitance
(a) interelectrode capacitors in a transducer between the i'th electrode and all other electrodes
(b) Equivalent circuit (only two nearest neighbors are shown).

calculate the charge distribution on the electodes due to an incident acoustic wave. This charge distribution is due to the piezoelectric effect which is neglected for calculating the response of a transducer. The charge distribution is present even for grounded arrays, so one cannot simply use reciprocity to find the voltage induced on the array and then use that voltage to find the charge distribution. Once the charge distribution induced on an electrode by an incident surface wave is found, the normal mode equations are used to find the reflection and velocity shift of the surface wave [8,9].

Up to now, the reflection and velocity shift of surface acoustic waves from electrodes have only been calculated for infinitely long periodic arrays of electrodes. The second part of this thesis presents a method to calculate the reflection and velocity shift of surface acoustic waves for an electrode near the end of a finite length periodic array or for an electrode in a withdrawal weighted transducer. First the charge distribution on the electrodes due to an incident acoustic wave is calculated assuming the array is periodic. Then the unwanted electrodes are removed and the change in the charge distribution resulting from withdrawing the electrodes is calculated electrostatically. This charge distribution must exactly cancel the charge distribution due to the acoustic wave in the regions where an electrode has been withdrawn. The circuit model descibed earlier is ideal for calculating this electrostatic charge distribution. The total charge distribution on the non-periodic array due to an incident surface wave is given by the sum of the original charge distribution due to the acoustic wave and the change in the charge distribution resulting from withdrawing the electrodes. The total charge distribution is then used in the normal mode equations to calculate the

reflection and velocity shift of an electrode in the non-periodic array.

Once the reflection and velocity shift of surface acoustic waves from a single electrode have been calculated, the effects of all of the reflections and all of the velocity shifts from all of the electrodes must be combined. One method calculates a piezoelectric scatter matrix for each electrode in the array (figure 3b) [9,10]. The scatter matrix elements relate the surface waves leaving an electrode to the waves incident on the electrode. They can be calculated from the reflection and the velocity shift. The scatter matrices are then cascaded to give the reflection and phase shift for the entire array. Alternately, the periodic array of electrodes can be modeled as a transmission line with impedance mismatches and shunt susceptances at each electrode (figure 1c) [11,12]. The impedance mismatch and shunt susceptance can also be calculated from the reflection and the velocity shift. Transmission line theory is then used to calculate the reflection and phase shift of the acoustic waves from the entire array. A very similar approach is to model the periodic transducer as a transmission line with impedance mismatches and velocity "mismatches" at each electrode (figure 3d) [13]. This technique has the advantage over the transmission line with shunt susceptances in that the the impedance mismatch and velocity mismatch are equal to the reflection and velocity shift respectively. Each of these three approaches yields the same results.

(A)

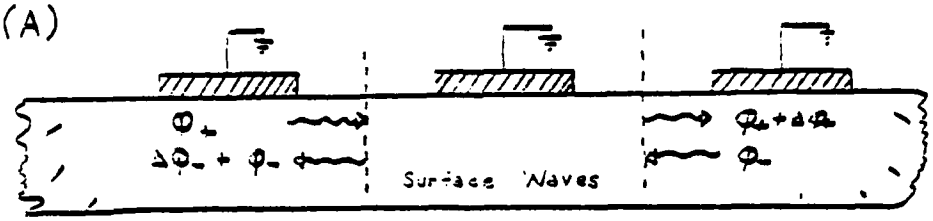

(B)

$$\begin{bmatrix} \Phi_- + \Delta\Phi_- \\ \Phi_+ + \Delta\Phi_+ \end{bmatrix} = \begin{bmatrix} S_{11} & S_{12} \\ S_{21} & S_{22} \end{bmatrix} \begin{bmatrix} \Phi_+ \\ \Phi_- \end{bmatrix}$$

(C)

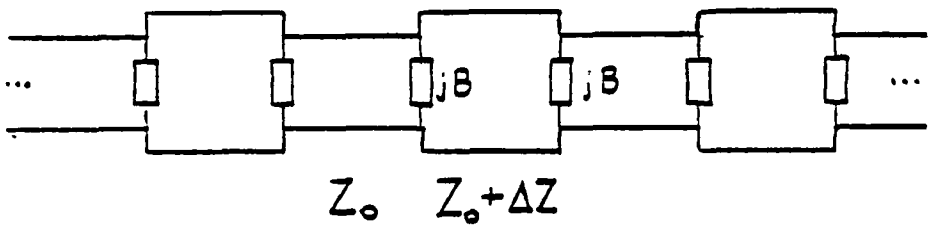

(D)

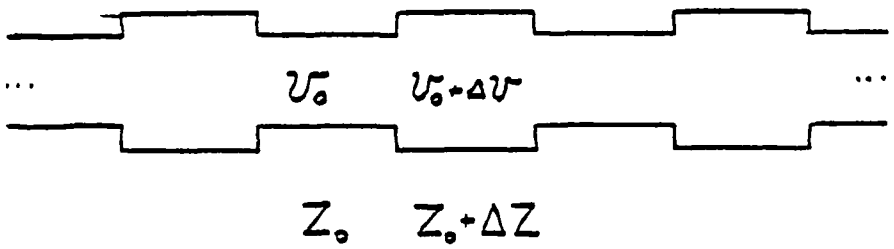

Figure 3: Modeling of SAW reflectors and transducers.
(a) Physical structure
(b) Scatter matrix model
(c) Transmission line model (shunt susceptance)
(d) Transmission line model (velocity change)

II. Transducer Analysis

The first step in finding the charge distribution for non-periodic transducers is to model the transducer by a periodic transducer consisting of many small electrodes and represent these electrodes by nodes in the circuit model (figure 1). The boundary conditions in the non-periodic transducer are replaced with the appropriate node excitations. For an unmetalized surface or gap, each node(small electrode) is driven by a zero current source(or is disconnected from all sources) to insure that the charge is equal to zero at every point on the surface. For a metalized surface, the nodes(small electrodes) are connected together,creating a supernode, so that the voltage is constant at every point on the surface. If the metalized surface is an electrode with a known tap weight, this supernode is connected to a voltage generator of that tap weight. If the metalized strip is unconnected (floating), then the supernode is connected to a zero current generator to insure that the electrode has a net charge of zero.

Figure 4 shows the potential distribution for a transducer with electrodes of alternating polarity modeled with four small electrodes per actual electrode and gap. The circles in the figure show the errors in the modeling process. As the density of small electrodes increases, the accuracy of the approximation increases. The density of the small electrodes is chosen in accordance with the range of spatial harmonics of interest. The small electrode spacing should be much less than one wavelength at the frequency of interest to insure that the charge distribution will be accurate. One should choose at least four small electrodes for the smallest electrode or gap in the non-periodic transducer

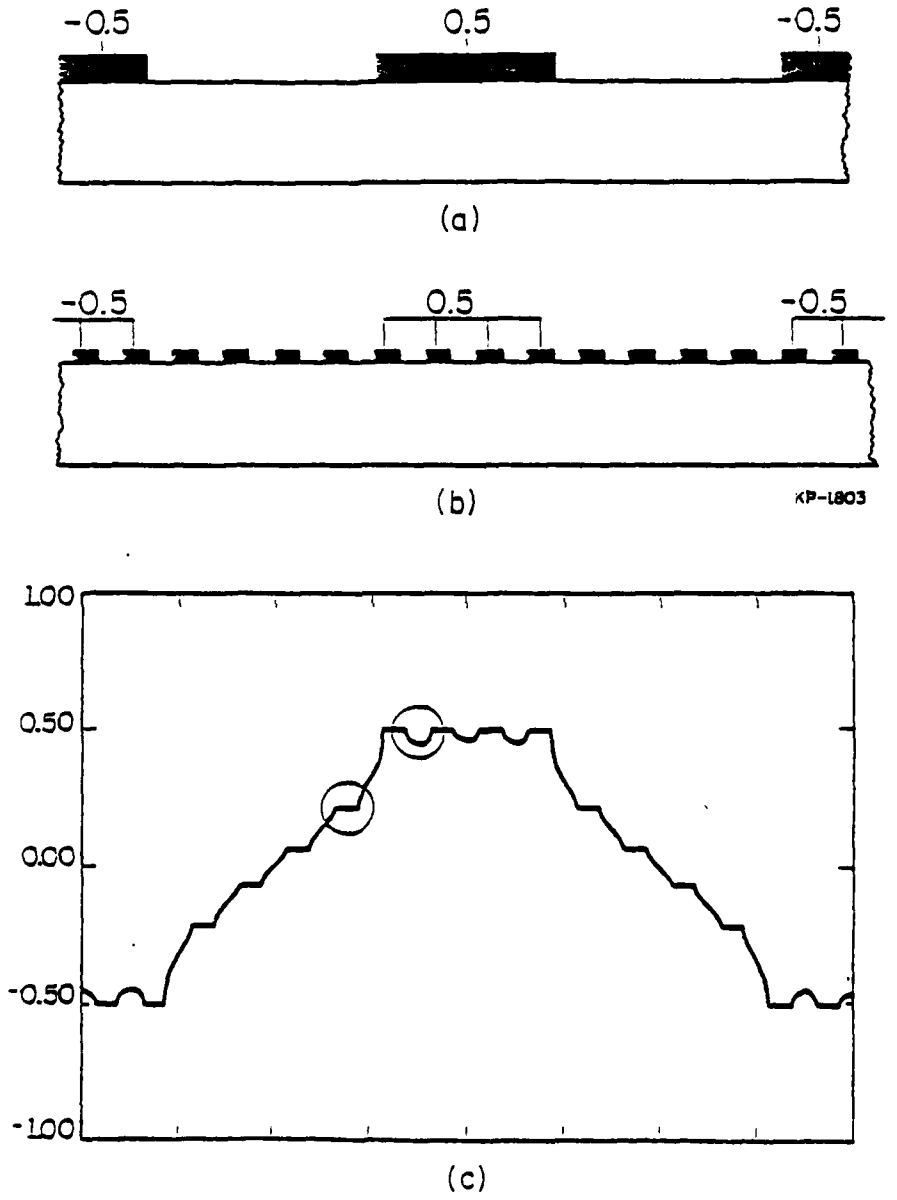

Figure 4: Potential and charge distribution for a single electrode transducer modeled with four small electrodes(divisions) per actual electrode and gap

(a) actual transducer
(b) modeling with small electrodes
(c) potential distribution

to calculate an accurate charge distribution at fundamental.

If many small electrodes are used, the potential and charge distributions will be independent of the duty factor, η, of the small electrodes. To verify this, the charge distribution in an infinite array consisting of electrodes with alternating polarities was calculated for different duty factors. The charge distributions look identical. The total charge on a single electrode was calculated by summing the charges on the small electrodes that are representing it. This charge varies only slightly as the duty factor of the small electrodes changes.(Δ in figure 5) It is also in good agreement with the theoretical value shown by the circle in the figure. A duty factor of 0.5 is chosen so that the very simple expression for the interelectrode capacitances can be used. These capacitances are represented by capacitors which are connected between the nodes.(figure 2) The value of the capacitor between the i'th and j'th node is:[4]

$$C_n = D \frac{1}{4n^2 - 1} \qquad n < m \qquad (1)$$

$$C_n = 0 \qquad n > m \qquad (2)$$

where :

$n = |i-j|$

m= number of nearest neighbors being considered

$D = \frac{4}{\pi}(\epsilon_p + \epsilon_0)$

W= beam width of the transducer

ϵ_p= effective dielectric constant of the substrate

ϵ_0= dielectric constant of free space

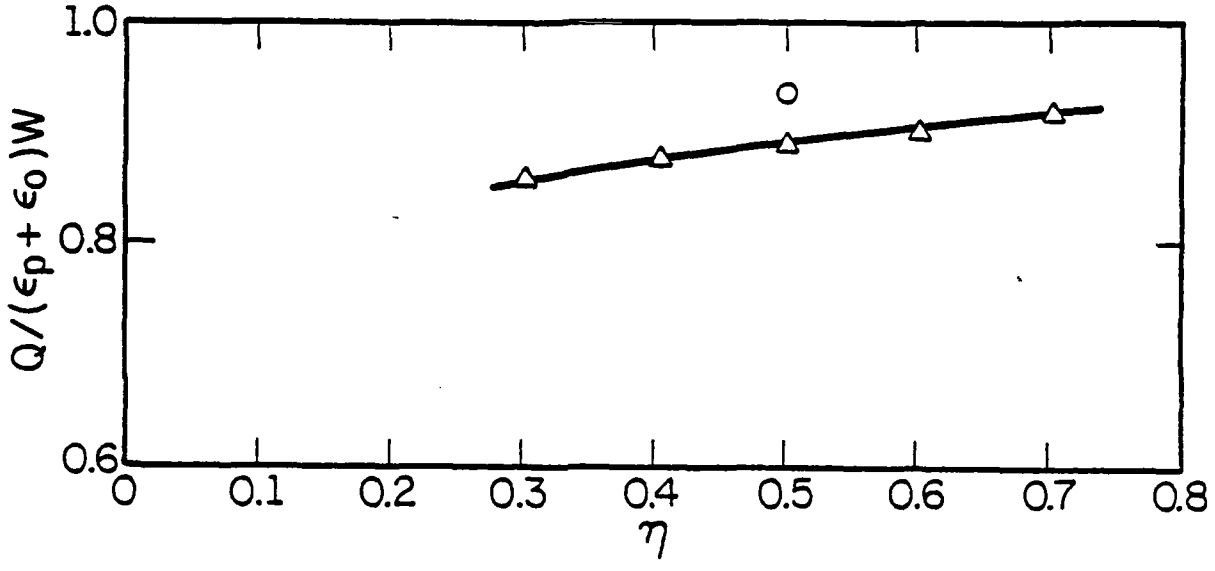

Figure 5: Total charge on one finger of an infinitely long single electrode transducer vs. the duty factor of the small electrodes that were used to calculate the charge distribution.

The dielectric constant at constant stress, ϵ_p^T, is used for the effective dielectric constant of the substrate [8].

The last step in the analysis of non-periodic transducers is to find the voltage and the net charge on each node. This is actually the charge on the capacitors connected to each node or the charge on each small electrode. The equation for the charge on the i'th node (small electrode) is given by:

$$Q_i = \sum_{j=-\infty}^{\infty} C_{|i-j|} (V_i - V_j) \qquad i \neq j \tag{3}$$

$$Q_i = V_i \left[\sum_{j=-\infty}^{\infty} C_{|i-j|} \right] - \sum_{j=-\infty}^{\infty} C_{|i-j|} V_j \qquad i \neq j \tag{4}$$

The equation for the charge on each tap can be written more simply as:

$$Q_i = \sum_{j=-\infty}^{\infty} D_{i-j} V_j \tag{5}$$

where :

$$D_0 = \sum_{n=-\infty}^{\infty} C_{|n|} \qquad n \neq 0 \tag{6}$$

$$D_n = D_{-n} = -C_n \qquad n \neq 0 \tag{7}$$

For a transducer with N small electrodes, the summation in equation 5 has N terms. End effects are taken into account by adding a few small floating electrodes at the end of the physical transducer structure and including them in the summation. The equations for the charge on each small electrode (node) are written in matrix form as:

$$\begin{bmatrix} Q_1 \\ Q_2 \\ \cdot \\ \cdot \\ \cdot \\ Q_N \end{bmatrix} = \begin{bmatrix} D_0 & D_{-1} & \cdots & D_{-(N-1)} \\ D_1 & D_0 & & \\ \cdot & & & \\ \cdot & & & \\ \cdot & & & \\ D_{N-1} & & & D_0 \end{bmatrix} \cdot \begin{bmatrix} V_1 \\ V_2 \\ \cdot \\ \cdot \\ \cdot \\ V_N \end{bmatrix} \qquad (8)$$

In general our matrix equation has N unknowns. They are:

(1) The voltages on the unconnected electrodes (nodes),

(2) The charges on the connected electrodes (nodes) with a known tap weight,

(3) The individual charges on the small electrodes (nodes) which represent a floating electrode and also the voltage on that floating electrode. However, since the sum of these individual charges is zero, there is still only one unknown per node.

This matrix equation is solved for the floating electrode voltages using a Gauss-Seidel Iteration technique [14]. Since the "D" matrix contains only N different elements, only the values of D_n need to be stored as opposed to N^2 elements to store the entire matrix.(see appendix I) Therefore a long non-periodic transducer can be analyzed without computer

memory limitations. A 150 electrode withdrawal weighted transducer, modeled with 4 divisions per electrode and gap requires 1200 small electrodes and 3 arrays of size 1200 to compute the charge distribution. On a Digital Equipment Co. DEC-10, this calculation takes less than four minutes with 64 nearest neighbors and a convergence within one percent . The details of this implementation are given in appendix I. Storage requirements are reduced even further for non-periodic transducers with a repeating section. This is shown in appendix II.

Once all of the node voltages have been found, the potential distribution for the transducer is simply the voltages on these nodes. The charge distribution for the transducer is given by the charge on each node divided by the period of the small electrodes (sampling rate). These charges are found using equation (5). The Fourier transform of the charge distribution is given by :

$$\sigma_T(f) = \sum_{n=1}^{N} Q_n e^{-j(2\pi f/v_s)np} \qquad (9)$$

where:

Q_n = charge leaving the n'th node

p = the small electrode spacing

v_s = the average surface wave velocity.

The admittance characteristics of the transducer are evaluated using equations (10-12). The radiation conductance Ga is given by [8]:

$$G_a(f) = 2\pi f \cdot W \epsilon_p \cdot \left(\frac{K^2}{2}\right) \cdot \left[\frac{\sigma_T(f)}{\epsilon_p W V_T}\right]^2 \qquad (10)$$

where :

K^2 = coupling coefficient

V_T = terminal voltage

The radiation susceptance Ba is given by [8]:

$$B_a(f) = \text{Hilbert Transform}\{G_a(f)\} \tag{11}$$

The transducer capacitance is given by [2]:

$$C_T = \sum_{n=1}^{N} \frac{Q_n}{V_T} T(n) \tag{12}$$

where N = number of small electrodes and

$$T(n) = \begin{cases} 1 & \text{if } V_n > 0 \\ 0 & \text{if } V_n \leq 0 \end{cases}$$

Once these admittance characteristics are known, the response of the transducer as a function of frequency can be calculated [8].

In figure 6 the potential distributions for infinite single and double electrode transducers calculated using this technique are compared to the known analytical distributions calculated from field theory. Notice that there is almost no difference between the the field thoery and circuit model results. Figure 7 shows the Fourier series representation of the potential and charge distributions for the double electrode transducer. Notice that the lower spatial harmonics are very accurate but there is some deviation at the higher harmonics. This is exactly what is expected because, at the higher harmonics, the electrode spacing is no longer much less than a wavelength.

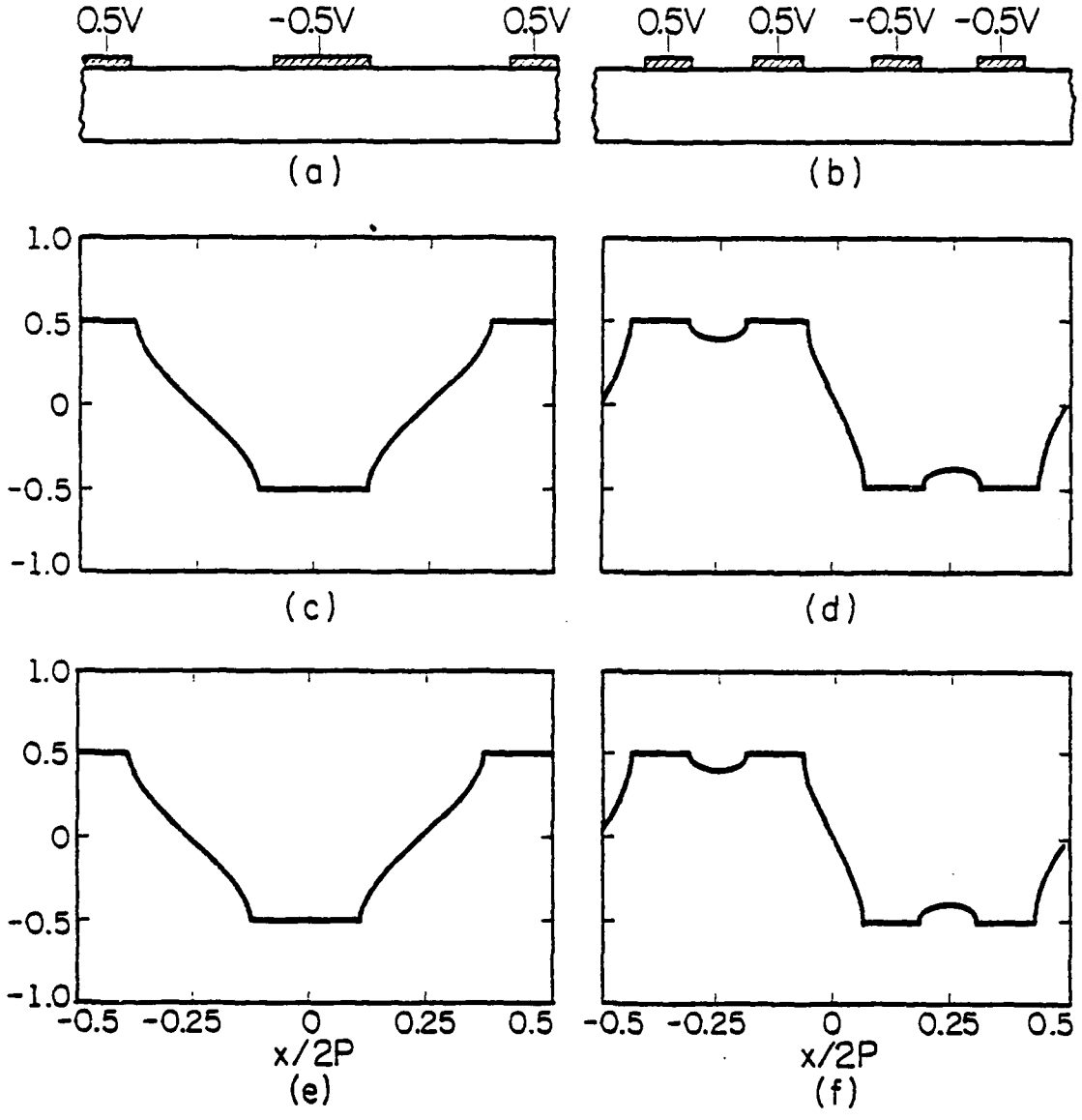

Figure 6: Potential distributions for single and double electrode transducers calculated using 16 divisions per electrode and calculated using field theory.

(a) Single electrode transducer structure
(b) Double electrode transducer structure
(c,d) potential distributions calculated using field theory
(e,f) potential distributions calculated using the circuit model

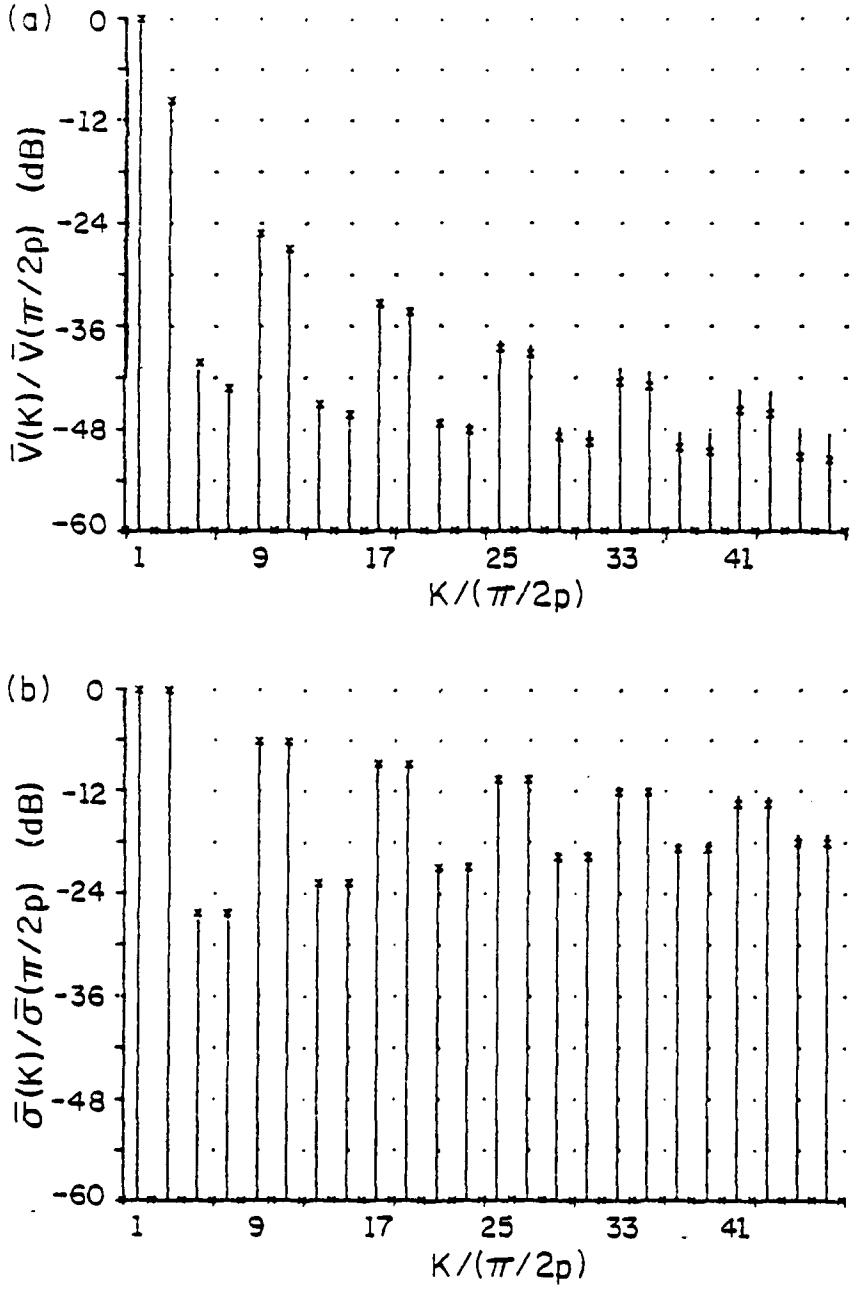

Figure 7: Spectral potential and charge distributions for a double electrode transducer calculated using this circuit model with 16 divisions per electrode and field theory distributions Bars correspond to the circuit model values and X's correspond to the field theory values. (duty factor is 31/64)

Figure 8 illustrates how to use the circuit model with an example of a non-periodic transducer, whose charge distribution is not analytically known. Figure 8a shows the repeating transducer structure to be analyzed. It is modeled with 2 small electrodes for every 1u in length, as shown in Figure 8b (a larger number may be used for greater accuracy). Then the equivalent circuit is drawn and the unknown node voltages are found. The potential distribution that is shown in Figure 8c is given by these node voltages. The charge distribution is found from equation (5) and shown in Figure 8d.

The technique that is used to find the charge distribution and response for an arbitrary non-periodic transducer is summarized below.

(1) Divide the transducer into many small electrodes.

(2) Draw the circuit model for these electrodes and apply the appropriate node equations.

(3) Solve for the node voltages to obtain the potential distribution.

(4) Find the charge on each node to obtain the charge distribution.

(5) Fourier transform the charge distribution to find $\overline{\sigma}_T(f)$.

(6) Use equations (10-12) to find the admittance characteristics, and hence the response of the transducer.

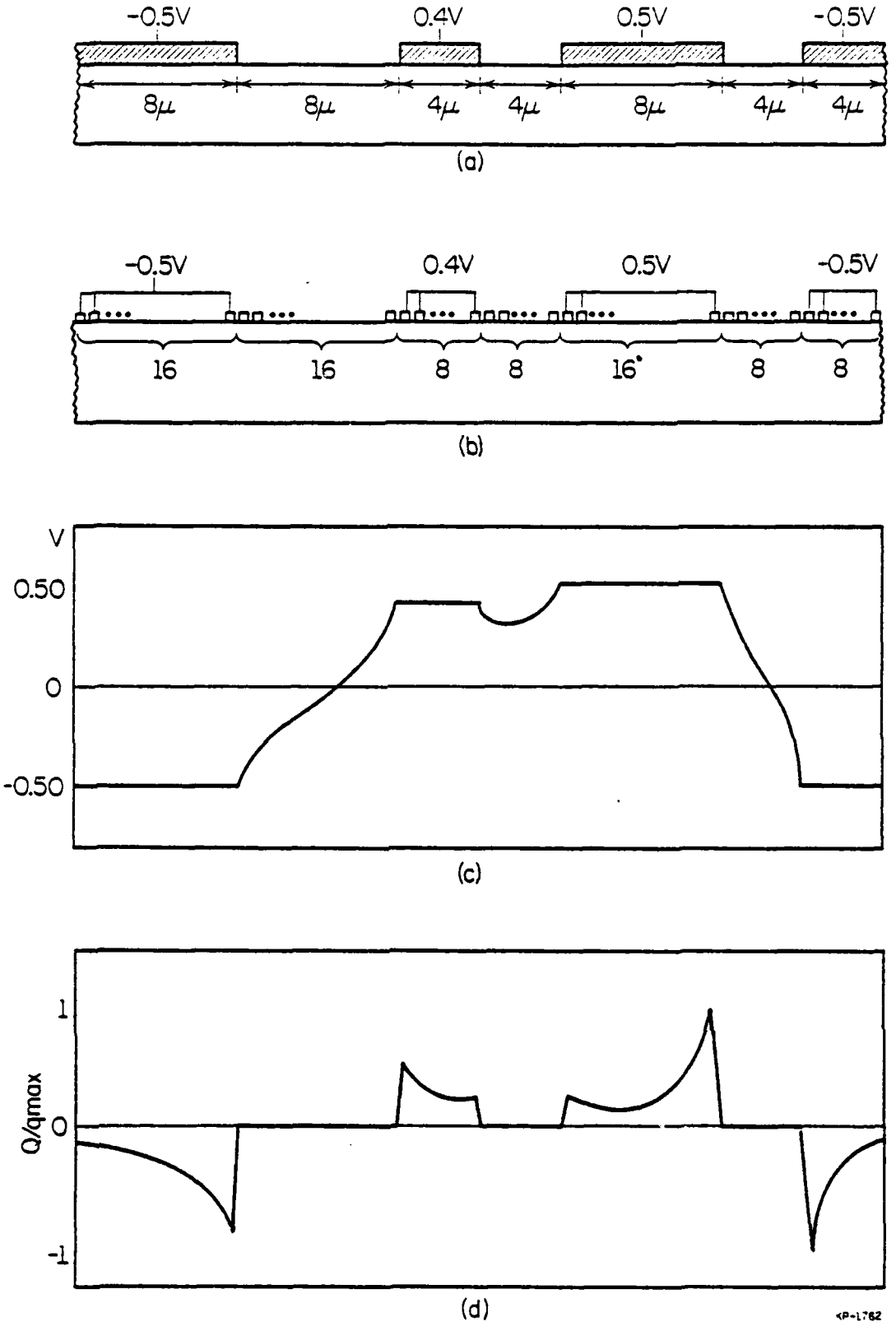

Figure 8: Non-peridic transducer
(a) actual transducer structure
(b) modeling with small electrodes
(c) potential distribution
(d) charge distribution

III. Reflector Analysis

To calculate the reflection and phase shift of surface acoustic waves from an array of electrodes one must calculate the reflection and velocity shift of surface acoustic waves from a single electrode and then combine the effects of all of the electrodes in the array. These reflections and velocity shifts are calculated using the normal mode approach [8]. First the charge distribution on an electrode due to an incident surface acoustic wave is calculated and then the reflection and velocity shift of the wave is calculated from that charge distribution. For infinitely long periodic arrays, this charge distribution, which is equal to the normal component of the electrical displacement at the surface (or D_y), can be calculated fairly easily [9]. This charge distribution is shown in figure 9b for an electrode spacing of one quarter wavelength (fundamental). In this graph, the phase reference is in the center of the first electrode and the exp(jwt) time dependence is taken out. If one electrode is removed, the problem of calculating the charge distribution is more difficult because the charge on all of the remaining electrodes will be different. The amount that the charge distribution on the electrodes changes when an electrode is withdrawn is determined by finding the electrostatic charge distribution on the electrodes which will add to the charge distribution on the electrodes due to the acoustic wave and leave a charge of zero on the surface where the electrode was withdrawn. Calculating this electrostatic charge distribution is very simple using the method outlined earlier in this thesis. The small electrodes, which represent an electrode that has been withdrawn, are driven with current sources(actually charge sources) which are equal to the opposite of the acoustic charge that it must cancel. The circuit equations used to find this charge distribution are identical

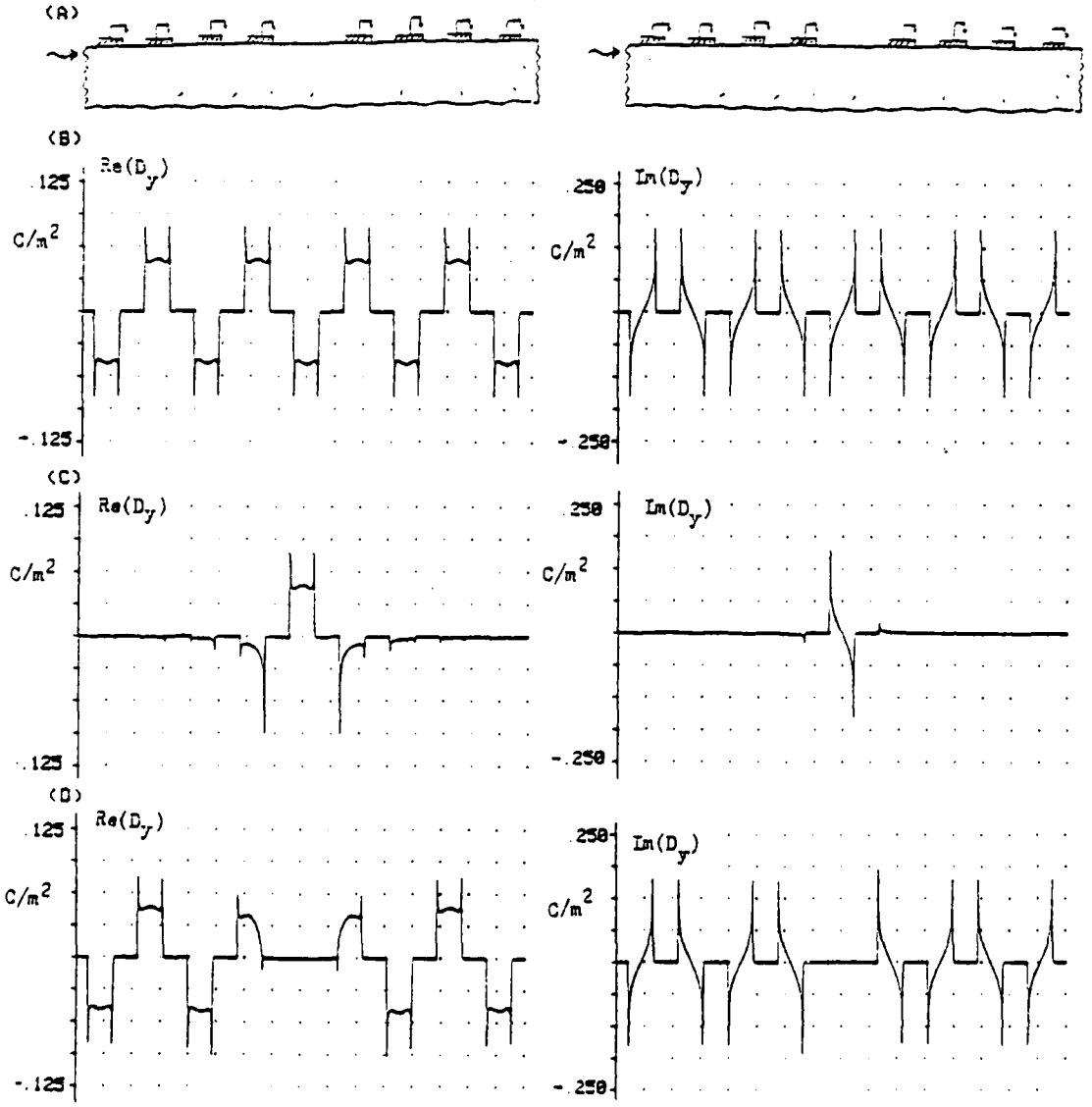

Figure 9: Charge distribution on a transducer or reflector with one electrode withdrawn due to an incident acoustic charge.

(a) Physical structure

(b) Real and imaginary parts of the charge distribution produced by an incident acoustic wave assuming all electrodes are present

(c) Real and imaginary parts of the electrostatic charge distribution produced by withdrawing one electrode.

(d) Real and imaginary parts of the charge distribution produced by an incident acoustic wave on the actual transducer structure

to the circuit equations used to find the charge distribution for a transducer except that these current(charge) sources give rise to the charge distribution instead of the voltage sources. This change in the charge distribution, resulting from withdrawing an electrode, is shown in figure 9c. The actual charge distribution due to an incident surface acoustic wave (figure 9d) is given by the sum of the original charge distribution (figure 9b) and the change in the charge distribution. Notice that the charge in the region where the electrode was withdrawn is equal to zero. Therefore the boundary conditions for the transducer are satisfied.

Once the charge distribution on each electrode is found, the reflection and velocity shift of any electrode in the array can be calculated. In reference 9 the reflection and velocity shift are calculated using the charge distribution for periodic transducers which is shown in figure 9b. To calculate the reflection and velocity shift of an electrode in an array with a withdrawn electrode, the charge distribution calculated in figure 9d is used instead. One should note that all of the electrodes near the missing electrode have different charge distributions and thus different values for reflection and velocity shift. However, the charge distribution for electrodes far from the withdrawn electrode is nearly the same as the charge distribution for an infinitely long periodic transducer. Therefore the reflection and velocity shift of these electrodes are identical to the reflection and velocity shift calculated for an infinitely long array.

For any electrode in an array with charge distribution, $D_y(\theta)$, the reflection and velocity shift are given by[9]:

$$r = \frac{\Delta \Phi_-}{\Phi_+} = \frac{-jp}{2\pi}\left(\frac{1}{\epsilon_p+\epsilon_0}\right)\left(\frac{K^2}{2}\right)\int_{-\pi}^{\pi} \frac{D_y(\theta)}{\Phi_+} e^{-j f_n \theta/2} \qquad (13)$$

$$\frac{\Delta V}{V} = \frac{1}{j\pi\eta}\frac{\Delta\Phi_+}{\Phi_+} = \frac{1}{\pi\eta}\cdot\frac{p}{2\pi}\left(\frac{1}{\epsilon_p+\epsilon_0}\right)\left(\frac{K^2}{2}\right)\int_{-\pi}^{\pi} d\theta\,\frac{D_y(\theta)}{\Phi_+}\,e^{f_n\theta/2}$$

where:

K^2 = coupling coefficient (14)

η = duty factor

p = electrode spacing

$\theta = \frac{2\pi x}{p}$

f_n = normalized frequency or $2 \cdot f \cdot p / v_s$

v_s = average surface wave velocity

The scatter matrix elements in figure 3b are given by (at fundamental) [9]:

$$S_{11} = S_{22} = r \tag{15}$$

$$S_{12} = S_{21} = 1 + j\,\pi\eta\,\frac{\Delta V}{V} \tag{16}$$

The impedance mismatch and shunt susceptance in figure 3c (at fundamental and a duty factor of 0.5) are given by:

$$\frac{\Delta Z}{Z} = r \tag{17}$$

$$jB = j(\pi/2)\,\frac{\Delta V}{V} \tag{18}$$

The impedance mismatch and velocity mismatch in figure 3d (at fundamental and a duty factor of 0.5) are given by:

$$\frac{\Delta Z}{Z_0} = r \tag{19}$$

$$\frac{\Delta V}{V_0} = \frac{\Delta V}{V} \tag{20}$$

As a check of the accuracy of this technique, consider an infinitely long periodic array of electrodes in which every other electrode is withdrawn. The reflection and velocity shift of surface waves from the remaining electrodes can be found using the technique presented in this paper (figure 10a) or using the previous theory for periodic transducers (figure 10b) [1]. The charge distribution on an electrode due to an incident acoustic wave from the left calculated using the technique presented in this paper is shown in figure 10c. The charge distribution calculated using the previous theory is shown in figure 10d. They are in good agreement. The reflection and velocity shift were also calculated using each of these techniques and their values are also in good agreement.

So far we have calculated the reflection and velocity shift of surface waves from an electrode in an array with only one withdrawn electrode and for an array with periodically withdrawn electrodes. The reflection and velocity shift can be calculated using this method when any number of electrodes are withdrawn in any order. In figure 11, three electrodes are withdrawn. Figure 11b shows the charge distribution due to the incident wave assuming all electrodes are present. Figure 11c shows the electrostatic charge distribution which is calculated by driving the transducer with a charge which will subtract from the acoustic charge to give a charge of zero in the regions where an electrode was withdrawn. Figure 11d shows the resulting total charge distribution. This charge distribution is used in equations 13 and 14 to calculate the reflection and velocity shift of the remaining electrodes.

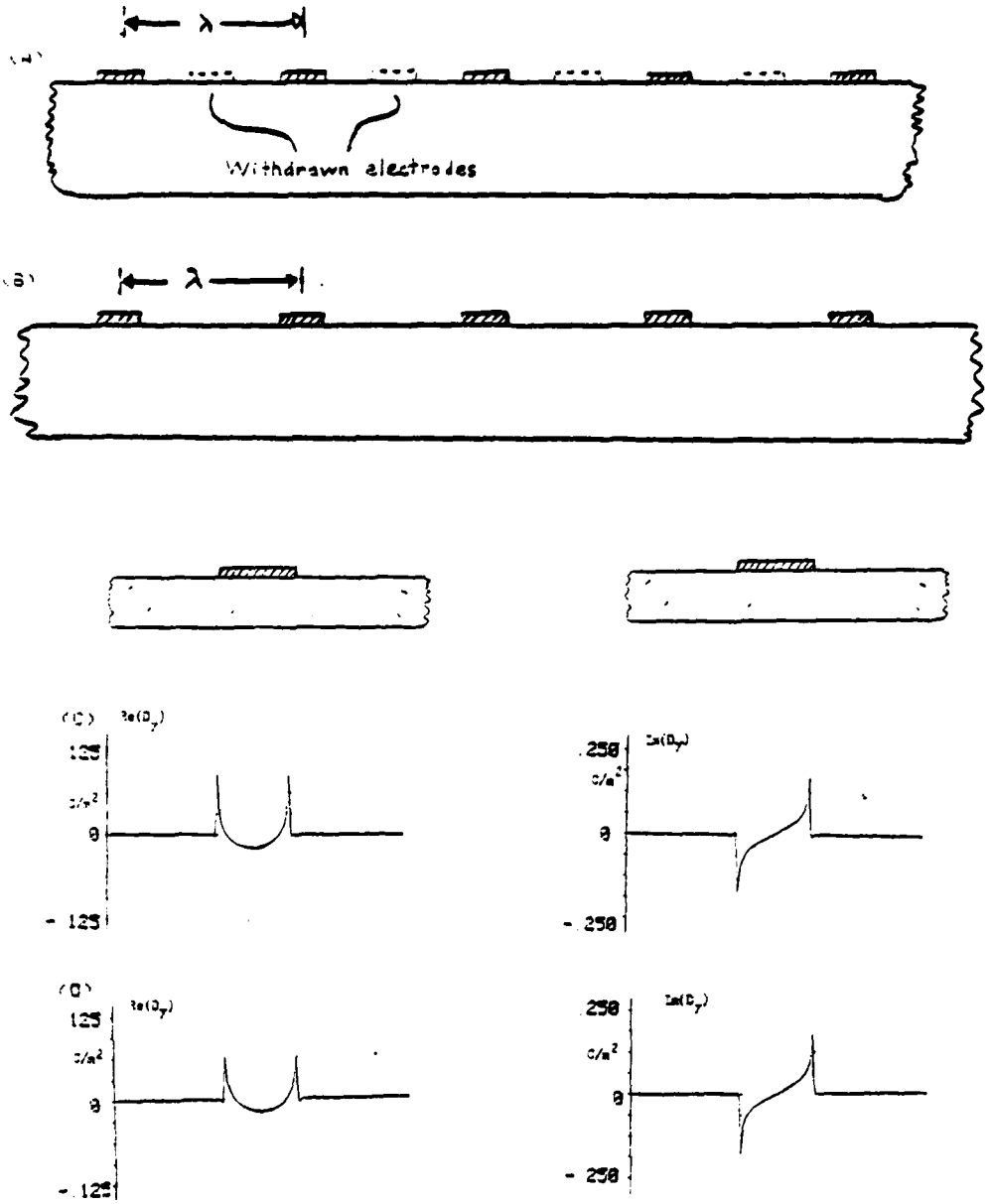

Figure 10: Charge distribution produced by an incident acoustic wave on a transducer with every other electrode removed.

(a) Physical structure showing withdrawn electrodes

(b) Same structure but thought of as a periodic structure with electrode spacing of one wavelength and duty factor of 0.25

(c) Real and imaginary parts of the charge distribution produced by an acoustic wave as calculated using the method presented in this paper

(d) Real and imaginary parts of the charge distribution produced by an incident acoustic wave as calculated using the previous theory for periodic transducers

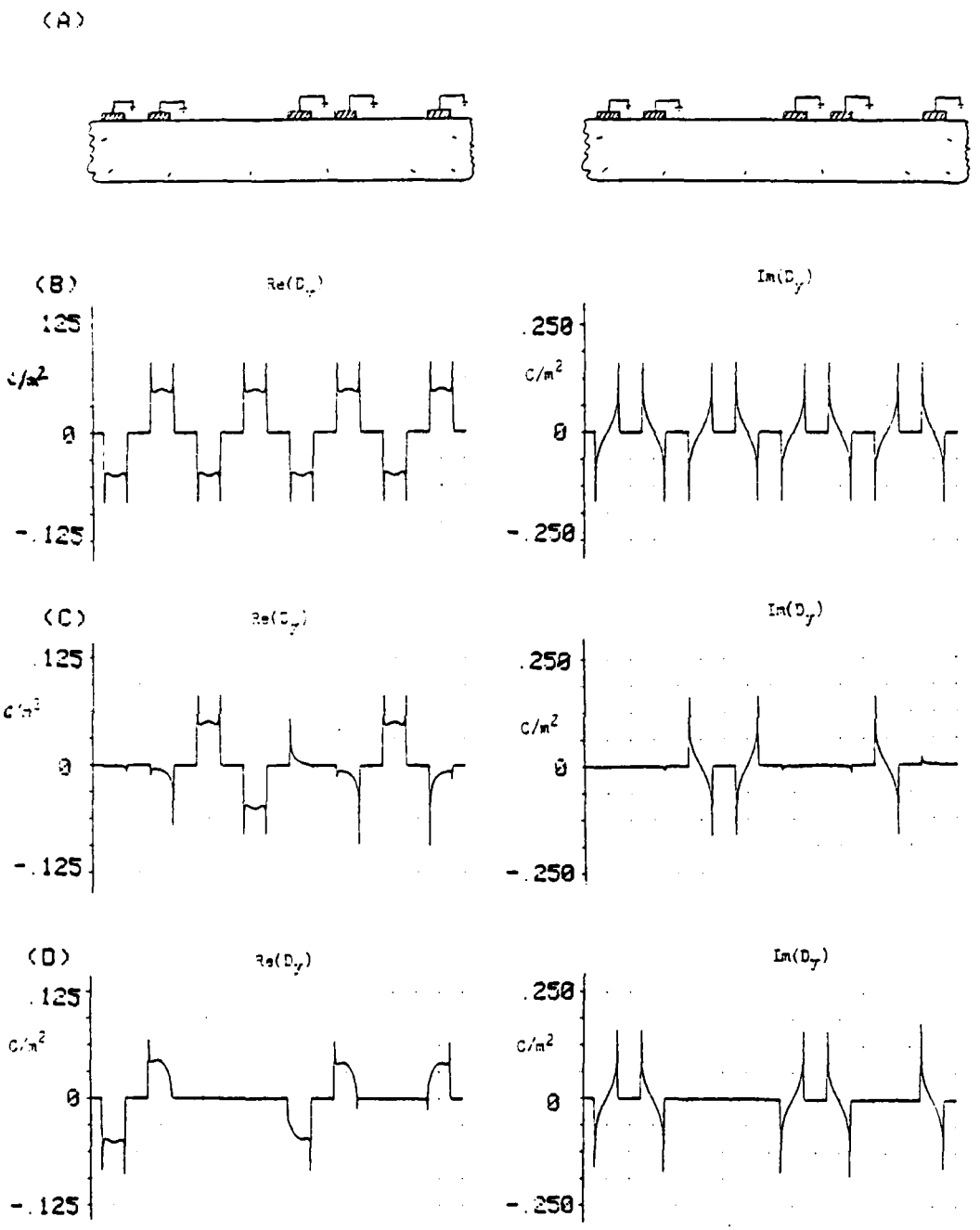

Figure 11: Charge distribution on a transducer or reflector with three electrodes withdrawn due to an incident acoustic charge.

(a) Physical structure

(b) Real and imaginary parts of the charge distribution produced by an incident acoustic wave assuming all electrodes are present

(c) Real and imaginary parts of the electrostatic charge distribution produced by withdrawing three electrodes

(d) Real and imaginary parts of the charge distribution produced by an incident acoustic wave on the actual transducer structure

For finite length peridic transducers or reflectors, the same technique is used to calculate the reflection and velocity shift of electrodes near the end of the transducer. Figure 12b shows the charge distribution for an infinitely long periodic transducer driven by an incident acoustic wave. The open surface at the end of the transducer is modeled as a series of withdrawn electrodes, and the resulting electrostatic charge distribution is found (figure 2c). The total charge is shown in figure 12d. In table 1 the reflection and velocity shift of electrodes near the end of a periodic transducer are tabulated at fundamental. The values of the reflection and the velocity shift for an electrode far from the end of the transducer are nearly equal to their values for an infinite periodic array.

The method used to calculate the reflection and phase shift for a withdawal weighted or finite length periodic array is summarized below.

(1) Determine the charge distribution on a single electrode due to an incident surface acoustic wave assuming all electrodes are present.

(2) Determine the electrostatic charge distribution which must cancel the original charge distribution in the regions where an electode is withdrawn.

(3) Sum these two charge distributions to get the actual charge distribution on the electrodes due to an incident acoustic wave.

(4) Use equations 13 and 14 to calculate the reflection and velocity shift of each individual electrode.

(5) Use equations 15-20 to determine either the scatter matrix elements or the transmission line parameters.

(6) Cascade the scatter matrices or use transmission line theory to calculate the reflection and phase shift for the entire transducer.

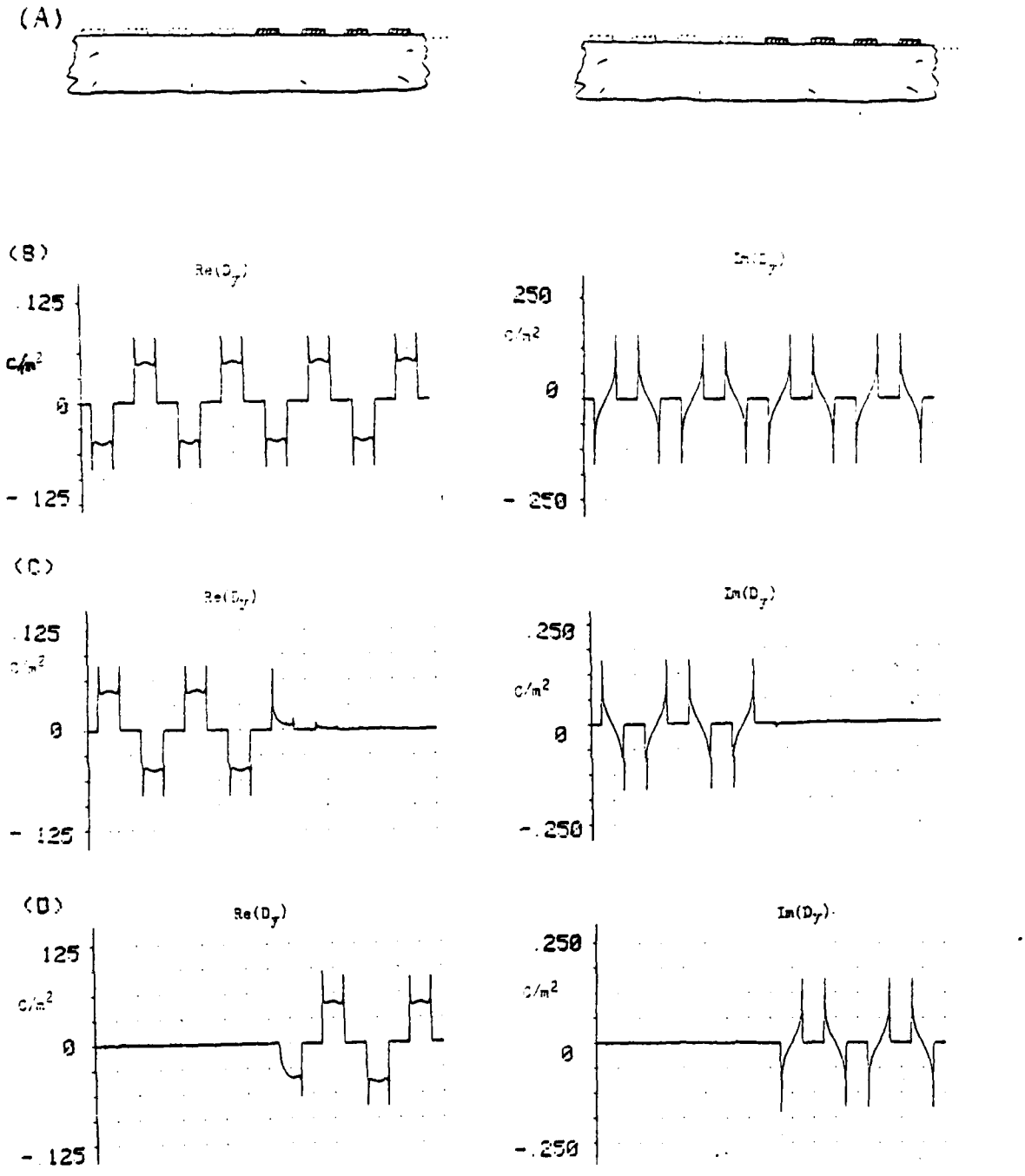

Figure 12: Charge distribution near the end of a periodic transducer or reflector due to an incident acoustic charge.

(a) Physical structure

(b) Real and imaginary parts of the charge distribution produced by an incident acoustic wave assuming all electrodes are present

(c) Real and imaginary parts of the electrostatic charge distribution produced by withdrawing the electrodes beyond the actual transducer structure

(d) Real and imaginary parts of the charge distribution produced by an incident acoustic wave on the actual transducer structure

Electrodes from the end of the transducer	$r / \frac{-2}{2}$	$\frac{\Delta v}{v} / \frac{K^2}{2}$
1	0.39	1.16
2	0.83	1.42
3	0.73	1.36
4	0.77	1.38
5	0.75	1.37
6	0.77	1.38
7	0.76	1.38
8	0.77	1.38
∞	0.76	1.38

Table 1: Reflection and velocity shift for electrodes near the end of a finite length periodic transducer

IV. Conclusion

This thesis presented a circuit model approach to calculate the electrostatic charge distribution for non-periodic surface acoustic wave transducers such as withdrawal weighted and chirped transducers. This charge distribution is then used to calculate the electrical port admittance parameters and the response of the transducer. The circuit model has been formulated in a way that allows long non-periodic transducers to be analyzed without computer memory limitations. Since reflectors cannot be analyzed using an electrostatic analysis, this thesis extended this method to calculate the reflection and velocity shift of surface acoustic waves for electrodes in withdrawal weighted arrays or for electrodes near the end of finite length periodic arrays. This method includes piezoelectricity only and neglects mechanical effects.

Appendix I

Solution of the matrix equation using a Gauss-Seidel iteration technique

Because of the symmetry of the circuit equations, a Gauss-Seidel iteration technique is used to find the unknown voltages on the floating electrodes. A Gaussian Elimination technique or matrix inversion technique requires that the entire matrix must be stored, thus requiring a large amount of computer memory [14]. Only the values of D_n need to be stored in this application of the Gauss- Seidel iteration technique. Using equation 5, the equation for the charge on the i´th electrode, if it is floating, is :

$$0 = \sum_{j=1}^{N} D_{i-j} V_j$$

This equation is solved for the voltage on the i´th electrode in terms of all other electrode voltages.

$$V_i = -\frac{1}{D_0} \left[\sum_{j=1}^{N} D_{i-j} V_j \Big|_{V_i = 0} \right]$$

Equation 14 is used to solve for the set of floating electrode voltages by first assuming that all of the floating electrode voltages are equal to zero and then recalculating them until their values converge to the correct ones. Figure 9 shows a flow chart of this process. Convergence is very rapid because D_{i-j} is small for $|i-j|$ greater than ten(tenth nearest neighbor). A rough estimate of the floating electrode voltages,and therefore the potential distribution, can be calculated quickly by choosing low density of small electrodes, only a few nearest neighbors, and a liberal tolerance on the convergence.

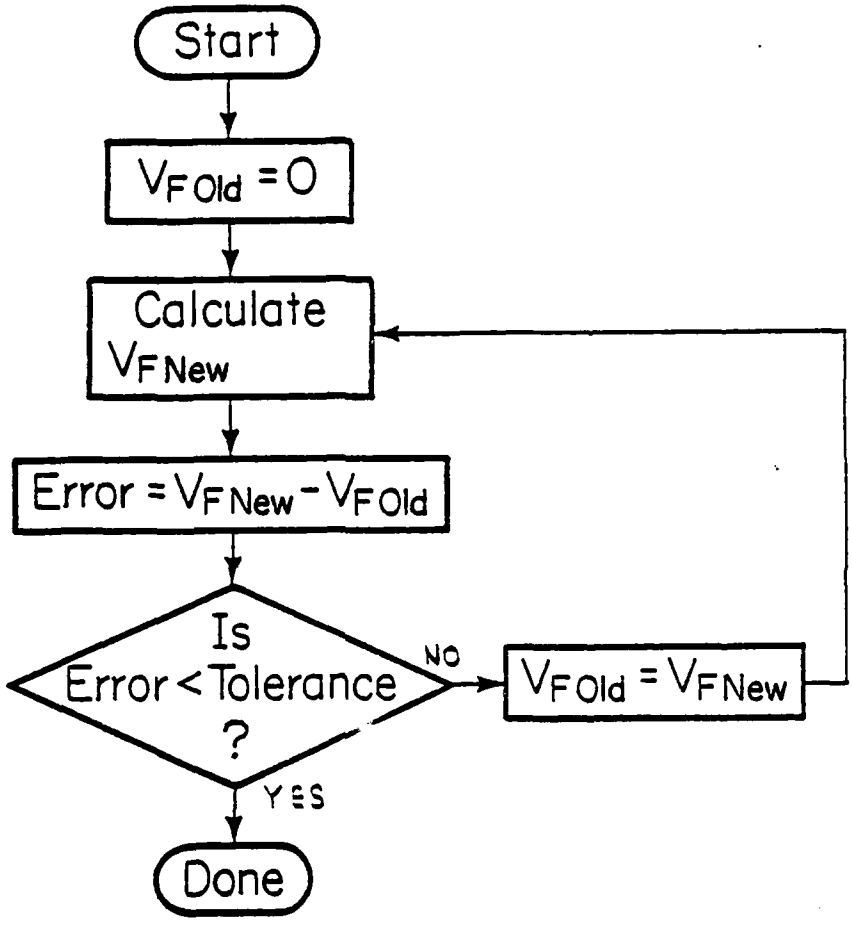

Figure 13: Flow chart of the Gauss-Seidel iteration technique applied to the solution of the floating electrode voltages.
(V_F =set of floating electrode voltages)

Appendix II Large Repeating Transducers

For large repeating arrays, a simplification can be made to reduce storage requirements further. Let N be the total number of small electrodes, n be the number of electrodes in the repeating section, and d be the number of sections in the transducer. From equation (5), the charge on any electrode is given by:

$$Q_i = \sum_{j=1}^{N} D_{i-j} V_j \tag{21}$$

However, since the voltages repeat with a period of n, this equation reduces to:

$$Q_i = \sum_{K=-\frac{d-1}{2}}^{\frac{d-1}{2}} \sum_{j=1}^{n} D_{i-j+Kn} V_j \tag{22}$$

$$Q_i = \sum_{j=1}^{n} \left[\sum_{K=-\frac{d-1}{2}}^{\frac{d-1}{2}} D_{i-j+Kn} \right] V_j \tag{23}$$

$$Q_i = \sum_{j=1}^{n} D'_{i-j} V_j \tag{24}$$

The value of D_{i-j} in equations 5 and 8 must now be replaced by D'_{i-j} from equation 24 . Only the values of D'_{i-j} need to be stored in the computer memory. If a transducer has ten repeating sections, this tech-

nique gives a tenfold reduction in the amount of computer memory required. The procedure for finding the potential and charge distribution is the same as previously described.

References

1. B. J. Hunsinger, "A generalized model for periodic transducers with arbitrary voltages," 1978 IEEE Ultrasonics Symposium Proceedings, pp. 705-708

2. S. Datta, B. J. Hunsinger and D. C. Malocha, "A generalized model for periodic transducers with arbitrary voltages," IEEE Transactions on Sonics and Ultrasonics, May 1979, pp. 235-242.

3. B. Lewis, P. M. Jordan, R. F. Milson and D. P. Morgan, "Charge and field superposition methods for analysis of generalized SAW interdigital transducers," 1978 IEEE Ultrasonics Symposium Proceedings, pp. 709-714.

4. S. Datta and B. J. Hunsinger, "Element factor for periodic transducers," IEEE Transactions on Sonics and Ultrasonics, Jan 1980.

5. C. S. Hartmann and B. G. Secrest, "End effects in interdigital surface wave transducers," 1972 IEEE Ultrasonics Symposium Proceedings, pp. 413-416.

6. W. R. Smith and W. F. Pedler, "Fundamental and harmonic frequency circuit model analysis of interdigital transducers with arbitrary metalization ratios and polarity sequence," IEEE Trans. Microwave Theory Tech., vol. MTT-23, pp. 853-864.

7. K. R. Laker, E. Cohen and A. J. Slobodnik, Jr., "Electric field interactions within finite arrays and the design of withdrawal weighted SAW filters at fundamental and higher harmonics," 1976 IEEE Ultrasonics Symposium Proceedings, pp. 317-321.

8. B. A. Auld, Acoustic Waves and Fields in Solids, vol. II,

John Wiley and Sons, 1973, pp. 170-175.

9. S. Datta and B. J. Hunsinger, "An analytical theory for the scattering of SAW by a single electrode in a periodic array on an anisotropic piezoelectric substrate," to be published in Journal of Applied Physics.

10. C. M. Panasik, "Scatter matrix analysis of surface acoustic wave reflectors and transducers," PhD. Thesis, University of Illinois at Urbana-Champaign, February 1980.

11. T. Aoki and S. Hattori, "Equivalent circuit parameteers for harmonic operation of SAW transducers," 1977 IEEE Ultrasonics Symposium Proceedings,. pp. 653-658

12. R. C. Li and J. Melngailis, "The influence of stored energy at step discontinuities on the behavior of surface wave gratings," IEEE Transactions on Sonics and Ultrasonics ., vol. SU-22, pp. 189-198, May 1975.

13. A. J. Slobodnik, Jr., K. R. Laker, T. L. Szabo, W. J. Kearns and G. A. Roberts, "Low sidelobe SAW filters using overlap and withdrawal weighted transducers," 1977 IEEE Ultrasonics Symposium Proceedings, pp. 757-762.

14. C. F. Gerald, Applied Numerical Analysis, Adison-Wesley Publishing Company, 1973, pp. 154-157.